

## Functionalization of Au surfaces with 4-(carboxymethyl)aniline and amine-terminated dendrimers for enhanced surface density of antibodies on immunosensor Au chips

Yongwoon Lee<sup>1</sup>, Youngwon Ju<sup>1</sup>, and Joohoon Kim<sup>1,2,\*</sup>

<sup>1</sup>Department of Chemistry, Research Institute for Basic Sciences, Kyung Hee University, Seoul 02447, Korea

<sup>2</sup>KHU-KIST Department of Converging Science and Technology, Kyung Hee University, Seoul 02447, Korea

(Received January 31, 2017; Revised February 9, 2017; Accepted February 9, 2017)

**Abstract:** Here, we demonstrate surface functionalization of Au chips with 4-(carboxymethyl)aniline (CMA) and amine-terminated polyamidoamine (PAMAM) dendrimers for immobilization of antibodies on the Au surfaces. Use of the functionalization strategy led to high surface density of the immobilized antibodies on the Au chips. Specifically, we found that the functionalization of Au chips with CMA and amine-terminated 6<sup>th</sup> generation PAMAM dendrimers allowed immobilization of immunoglobulin (IgG) antibodies with high surface density, which is 5 times higher than that obtained with Au surfaces functionalized with CMA and ethylenediamine.

**Key words:** 4-(Carboxymethyl)aniline, Dendrimer, Surface density of antibodies, Immunosensor Au chip

### 1. Introduction

Functionalization of electrode surfaces is of particular interest in the research of electrochemical immunosensor chips because it is a crucial step to immobilize fragile sensing elements, usually antibodies, appropriately on the immunosensor chips.<sup>1,2</sup> The surface functionalization is thus directly related to the analytical performances of the immunosensor chips.<sup>3</sup> Especially, the surface density of immobilized sensing elements is one of the critical features affecting the analytical performances obtained.<sup>4,5</sup> Thus, many promising strategies have been suggested to obtain precise immobilization of the biological sensing

molecules with high surface density of the immobilized molecules on chips surfaces.<sup>6-8</sup> Of the strategies, electrografting methods have been demonstrated for the surface functionalization and subsequent immobilization of biological molecules on a variety of electrode surfaces such as carbon, metals, indium tin oxide (ITO), and diamond.<sup>9-13</sup> For example, the use of aryl diazonium cation has been suggested to perform a direct electrochemical grafting at the surface of conducting electrodes.<sup>3,14,15</sup> Recently, our group also reported the electrochemical grafting of amine-terminated dendrimers on electrode surfaces.<sup>16-18</sup>

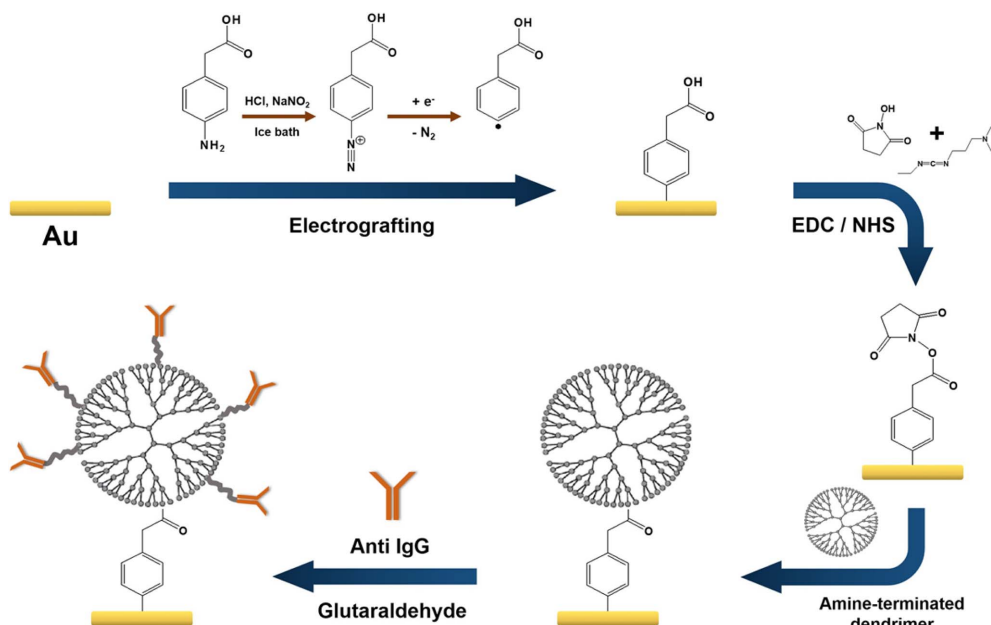
In this study, we report surface functionalization of Au electrodes with 4-(carboxymethyl)aniline (CMA)

★ Corresponding author

Phone : +82-(0)2-961-9384; Fax : +82-(0)2-961-0443

E-mail : jkim94@khu.ac.kr

This is an open access article distributed under the terms of the Creative Commons Attribution Non-Commercial License (<http://creativecommons.org/licenses/by-nc/3.0>) which permits unrestricted non-commercial use, distribution, and reproduction in any medium, provided the original work is properly cited.



Scheme 1. Schematic illustration of the surface functionalization of Au with CMA and amine-terminated PAMAM dendrimers for immobilization of antibodies.

and amine-terminated polyamidoamine (PAMAM) dendrimers for immobilization of antibodies on the Au surfaces, allowing high surface density of the immobilized antibodies (Scheme 1). Specifically, we functionalized Au surfaces with CMA via the electrografting process of the aniline derivative to introduce carboxyl moieties on the Au surfaces. The electrografting process consists of diazotation reaction of the aniline derivative, leading to the formation of an aryl diazonium cation, and the subsequent electrochemical reduction of the formed aryl diazonium species generating an aryl radical. The generated aryl radical attacks the Au surfaces, resulting in the covalent grafting to the Au surface (i.e., denoted as CMA-functionalized Au). Amine-terminated  $n^{\text{th}}$  generation PAMAM dendrimers ( $Gn-NH_2$ ,  $n = 4$  and  $6$ ) were then conjugated to the introduced carboxyl groups on the CMA-functionalized Au surface via amine – *N*-hydroxysuccinimide (NHS) coupling chemistry, which resulted in the formation of Au electrode functionalized with CMA and  $Gn-NH_2$  ( $n = 4$  and  $6$ ) (i.e., denoted as  $Gn-NH_2$ /CMA-functionalized Au,  $n = 4$  and  $6$ ). Importantly, we found that

the use of  $G6-NH_2$ /CMA-functionalized Au allowed immobilization of immunoglobulin (IgG) antibodies with high surface density, which is 5 times higher than that obtained with Au surfaces functionalized with CMA and ethylenediamine.

## 2. Experimental

### 2.1. Reagents and materials

Amine-terminated  $n^{\text{th}}$  generation PAMAM dendrimers ( $Gn-NH_2$ ,  $n = 4$  and  $6$ ), ethylenediamine, 4-(carboxymethyl)aniline (CMA), *N*-hydroxysuccinimide (NHS), 1-ethyl-3-(3-dimethyl-aminopropyl) carbodiimide (EDC), ethanolamine, 4-morpholineethanesulfonic acid (MES),  $K_3Fe(CN)_6$ ,  $Ru(NH_3)_6Cl_3$ ,  $NaNO_2$ ,  $LiClO_4$ , glutaraldehyde, phosphate-buffered saline (PBS), anti-mouse immunoglobulin (IgG) antibodies were purchased from Sigma-Aldrich, Inc. (USA).  $H_2SO_4$  and HCl were obtained from Daejung, Inc. (Korea). Bare Au chips were obtained from Biosensing Instrument (USA) for surface plasmon resonance (SPR) measurements. 18 M $\Omega$ -cm deionized (DI) water was used in the preparation of aqueous solutions

(aquaMAX Ultra370, YL Instrument Co., Ltd., Korea).

## 2.2 Functionalization of Au surfaces with CMA and amine-terminated PAMAM dendrimer

The electrografting of CMA on Au electrodes was performed using the previously reported methods with some modification.<sup>3,15</sup> Briefly, 20 mM CMA was diazotated in an aqueous solution containing 15 mM HCl and 15 mM NaNO<sub>2</sub> for 20 min under stirring in an ice bath. Cleaned Au electrodes were immediately immersed in the formed diazonium solution. The potential of the immersed Au electrodes was then cycled between 0.0 and -1.2 V (vs. Ag/AgCl). After the electrografting process, the Au electrodes were rinsed thoroughly with DI water and subsequently ultrasonicated in DI water for 3 min to remove any unbound molecules. The resulting CMA-functionalized Au electrodes were then immersed in 0.1 M MES buffer solution (pH 6.8) containing 0.1 M EDC and 0.1 M NHS for 1 h to activate the carboxyl moieties on the CMA-functionalized Au. After washing out the activated CMA-functionalized Au electrodes with DI water, immobilization of amine-terminated PAMAM dendrimers was achieved with drops of aqueous 100 μM *Gn*-NH<sub>2</sub> ( $n = 4$  and  $6$ ) solutions directly deposited on the surface of the CMA-functionalized Au for 4 h. After the immobilization of PAMAM dendrimers, the electrodes were rinsed with DI water and then placed in a blocking solution (0.1 M ethanolamine in 0.1 M MES buffer (pH 6.8)) for 30 min. Finally, the resulting *Gn*-NH<sub>2</sub>/CMA-functionalized Au electrodes ( $n = 4$  and  $6$ ) were washed with DI water, ultrasonicated thoroughly in DI water for 5 min, and blown until dry.

## 2.3 Immobilization of anti-mouse IgG antibodies on the surface of *Gn*-NH<sub>2</sub>/CMA-functionalized Au ( $n = 4$ and $6$ )

For immobilization of anti-mouse IgG antibodies, bare Au chips for SPR measurements were subjected to the surface functionalization with CMA and amine-terminated  $n^{\text{th}}$  generation dendrimers (*Gn*-NH<sub>2</sub>,  $n = 4$  and  $6$ ) as described earlier. The *Gn*-NH<sub>2</sub>/CMA-functionalized Au chips were incubated with

drops of 10 mM PBS buffer solution (pH 7) containing 1 % glutaraldehyde and 1 mM NaBH<sub>3</sub>CN for 1 h, and then rinsed with DI water thoroughly. The resulting Au chips were then subjected to SPR measurements by flowing 30 μg/mL anti-mouse IgG in 10 mM PBS buffer containing 1 mM NaBH<sub>3</sub>CN on the surface of Au chips.

## 2.4. Instrumentation and measurements

Electrochemical experiments were performed with a Model 440 potentiostat (CH Instruments, USA) using a conventional three-electrode electrochemical cell containing Au working electrodes. Before the electrochemical measurements, Au electrodes were polished with 0.3 μm alumina powders on a polishing pad (Buehler, USA) and rinsed with DI water. Any residual alumina powders were removed by ultrasonating the Au electrodes successively in ethanol and DI water. The polished Au electrodes were then subjected to the electrochemical cleaning by cycling the electrode potential in 0.5 M H<sub>2</sub>SO<sub>4</sub> between 0.0 and 1.5 V (vs. Ag/AgCl) until steady cyclic voltammograms (CVs) were obtained. A Pt wire and a Ag/AgCl (3 M NaCl) electrode were used as a counter and a reference electrode, respectively. SPR measurements were carried out using a Bi-4000 instrument (Biosensing Instrument, USA).

## 3. Results and Discussion

### 3.1. Electrochemical grafting of CMA on Au surfaces

Au electrodes were used as well-characterized substrates of immunosensor chips to study the surface density of immobilized antibodies on the Au surfaces. First, Au electrodes were mechanically and electrochemically cleaned to ensure the well-characterized and reproducible condition of the Au surfaces (see the Experimental section for experimental details). In brief, the Au electrodes were mechanically polished using fine-sized alumina powders (0.3 μm) and electrochemically cleaned by applying consecutive potential cycles in 0.5 M H<sub>2</sub>SO<sub>4</sub> solution. This cleaning process resulted in the formation of the

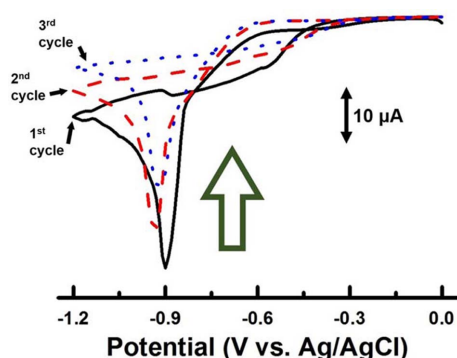


Fig. 1. CVs of 4-(carboxymethyl)benzenediazonium on an Au electrode in an aqueous solution containing 20 mM CMA, 15 mM HCl, and 15 mM NaNO<sub>2</sub>. Scan rate: 10 mV/s.

well-characterized Au surfaces reproducibly. After the cleaning process, the Au electrodes exhibited steady CVs showing the characteristic electrochemical redox peaks of Au, which indicates the well-characterized and reproducible Au surface.<sup>19,20</sup>

After ensuring the condition of Au surfaces, the electrochemical grafting of CMA at the Au surfaces was investigated by adaptation of the procedures reported previously for the functionalization of graphite electrodes with aniline derivatives.<sup>3,15</sup> Specifically, the potential of the cleaned Au electrodes was cycled multiple times between 0.0 and -1.2 V (vs. Ag/AgCl) in aqueous solutions containing diazonium cations (see the Experimental section for experimental details). Fig. 1 shows CVs obtained during the three consecutive cycles at a scan rate of 10 mV/s. The first cycle shown in Fig. 1 exhibits a well-defined and irreversible reduction peak at ca. -0.9 V (vs. Ag/AgCl). This reduction peak corresponds to the typical electrochemical reduction wave of the diazonium cations, resulting in the elimination of N<sub>2</sub> molecules and the formation of aryl radicals.<sup>15</sup> The aryl radicals were known to attack the Au surface and to form a covalent bond between the aryl group and the Au surface.<sup>15,21,22</sup> When the potential cycle was consecutively repeated (i.e., the second and the third cycles in Fig. 1), the reduction currents gradually decreased, indicating the irreversible formation of the aryl group layer and the gradual surface saturation of the molecular layer on the Au surface.

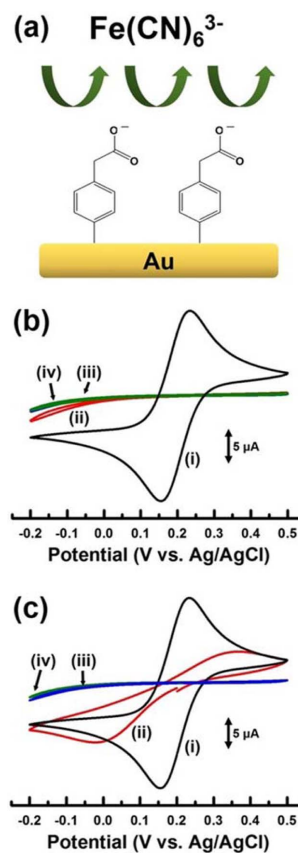


Fig. 2. (a) Illustration of negatively charged Fe(CN)<sub>6</sub><sup>3-</sup> on a CMA-functionalized Au in 0.1 M LiClO<sub>4</sub> (pH 7). (b) CVs of 5 mM Fe(CN)<sub>6</sub><sup>3-</sup> in 0.1 M LiClO<sub>4</sub> solution (pH 7) on (i) a bare Au electrode and (ii, iii, and iv) CMA-functionalized Au electrodes obtained after the application of the different number of potential cycles ((ii) 3 cycles, (iii) 5 cycles, and (iv) 10 cycles) at a scan rate of 10 mV/s for the electrografting of CMA. (c) CVs of 5 mM Fe(CN)<sub>6</sub><sup>3-</sup> in 0.1 M LiClO<sub>4</sub> solution (pH 7) on (i) a bare Au electrode and (ii, iii, and iv) CMA-functionalized Au electrodes obtained after the application of the potential cycles (3 cycles) at different scan rates ((ii) 200, (iii) 10, and (iv) 1 mV/s) for the electrografting of CMA. Scan rate: 20 mV/s.

The extent of the layer formation on the CMA-functionalized Au electrodes was further probed by cyclic voltammetry since cyclic voltammetry is an effective technique for studying the feature of surface-modified electrodes.<sup>23</sup> Especially, we evaluated the effects of experimental parameters, including the number of potential cycles and the scan rates applied during the electrografting process, on the extent of the

layer formation on the CMA-functionalized Au electrodes. As illustrated in *Fig. 2(a)*, we expected the carboxylic group of the electrografted CMA ( $pK_a = 3.8$ ) to be deprotonated in 0.1 M  $\text{LiClO}_4$  (pH 7), which prevents the penetration of the negatively charged redox probe  $\text{Fe}(\text{CN})_6^{3-}$  to the electrografted CMA layer depending on the extent of the layer formation. To evaluate the effect of the number of potential cycles applied, we cycled the potential of the cleaned Au electrodes different times (i.e., 3, 5, and 10 cycles) at a fixed scan rate of 10 mV/s in aqueous solutions containing diazonium cations. *Fig. 2(b)* shows the CVs of  $\text{Fe}(\text{CN})_6^{3-}$  in the  $\text{LiClO}_4$  solution on CMA-functionalized Au electrodes obtained after the application of the different number of potential cycles. For comparison, a CV of  $\text{Fe}(\text{CN})_6^{3-}$  on a bare Au electrode is also presented in *Fig. 2(b)*. The CVs clearly indicate the effective blocking of the penetration of  $\text{Fe}(\text{CN})_6^{3-}$  to the electrografted CMA layer, resulting in the nearly complete disappearance of the redox currents of  $\text{Fe}(\text{CN})_6^{3-}$  compared to that on the bare Au electrode. The substantial blocking was obtained even with the application of three potential cycles, suggesting that the three potential cycles applied was enough to achieve the surface saturation of the electrografted CMA layer on the Au electrodes. We also evaluated the effect of the scan rates applied during the electrografting process. *Fig. 2(c)* shows the CVs of  $\text{Fe}(\text{CN})_6^{3-}$  in the  $\text{LiClO}_4$  solution on CMA-functionalized Au electrodes obtained after cycling potentials three times at different scan rates (i.e., 200, 10, and 1 mV/s). The CVs also exhibited the nearly complete blocking of the penetration of  $\text{Fe}(\text{CN})_6^{3-}$  to the electrografted CMA layer obtained with sufficiently low scan rates (i.e., 10 and 1 mV/s). Those results suggest that such fast electrografting process, for example, three potential cycles at a scan rate of 10 mV/s, could lead to the sufficient extent of electrografted CMA layer formation on the CMA-functionalized Au electrodes.

### 3.2. Further functionalization of CMA-functionalized Au surfaces with amine-terminated PAMAM dendrimer

After characterizing the electrografted CMA layer

on the Au surfaces, we further functionalized the CMA-functionalized Au electrodes with amine-terminated PAMAM dendrimers. Since the PAMAM dendrimers contains a number of terminal amine groups, the additional functionalization of the CMA-functionalized Au electrodes with the dendrimers would provide a high number of immobilized amine moieties on the Au surfaces. For example, amine-terminated 6<sup>th</sup> generation PAMAM dendrimers (G6-NH<sub>2</sub>) contain 256 amine groups at the terminals.<sup>24-26</sup> Thus, the further functionalization of the CMA-functionalized Au electrodes with the G6-NH<sub>2</sub> dendrimers would provide the high number of immobilized amine moieties, which can be used as conjugation sites for immobilization of antibodies on the Au surfaces. Specifically, we immobilized the G6-NH<sub>2</sub> dendrimers on CMA-functionalized Au electrodes via covalent coupling of the amine terminals of G6-NH<sub>2</sub> to the carboxylic group of the electrografted CMA, resulting in the formation of G6-NH<sub>2</sub>/CMA-functionalized Au electrodes. To confirm the

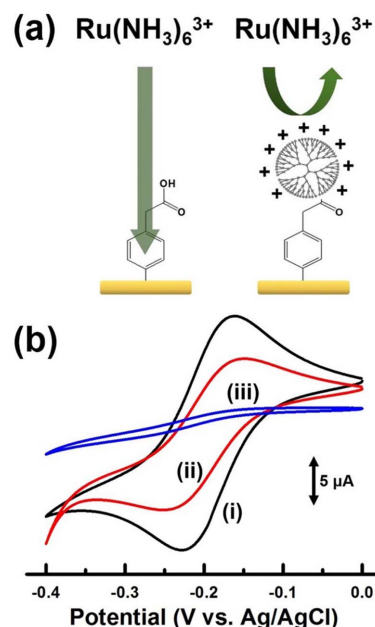


*Fig. 3.* (a) Illustration of positively charged  $\text{Ru}(\text{NH}_3)_6^{3+}$  on (left) a CMA-functionalized or (right) a G6-NH<sub>2</sub>/CMA-functionalized Au electrode in  $\text{H}_2\text{SO}_4$ . (b) CVs of 5 mM  $\text{Ru}(\text{NH}_3)_6^{3+}$  in 0.5 M  $\text{H}_2\text{SO}_4$  solution on (i) a bare, (ii) a CMA-functionalized, and (iii) a G6-NH<sub>2</sub>/CMA-functionalized Au electrode. Scan rate: 20 mV/s.

immobilization of the G6-NH<sub>2</sub> dendrimers on CMA-functionalized Au electrodes, we investigated the functionalized Au surfaces with a positively charged redox probe Ru(NH<sub>3</sub>)<sub>6</sub><sup>3+</sup> using cyclic voltammetry. As illustrated in Fig. 3(a), the G6-NH<sub>2</sub>/CMA-functionalized Au electrode is expected to be positively charged in 0.5 M H<sub>2</sub>SO<sub>4</sub> while the charge of CMA-functionalized Au surface is neutral, because terminal amine group (pK<sub>a</sub> = 9.5) of the G6-NH<sub>2</sub> and carboxylic group (pK<sub>a</sub> = 3.8) of the CMA are mostly protonated in the acidic solution.<sup>9</sup> Thus, the positively charged Ru(NH<sub>3</sub>)<sub>6</sub><sup>3+</sup> is expected to be repelled electrostatically from the G6-NH<sub>2</sub>/CMA-functionalized Au electrode while the CMA-functionalized Au electrode allows the approach of Ru(NH<sub>3</sub>)<sub>6</sub><sup>3+</sup>, which distinguishes the electrochemical behaviors of Ru(NH<sub>3</sub>)<sub>6</sub><sup>3+</sup> on the functionalized Au surfaces. Indeed, we observed substantial decrease in the redox currents of Ru(NH<sub>3</sub>)<sub>6</sub><sup>3+</sup> on the G6-NH<sub>2</sub>/CMA-functionalized Au electrode ((iii) in Fig. 3(b)) compared to those on bare Au electrode ((i) in Fig. 3(b)). However, we observed the redox currents of Ru(NH<sub>3</sub>)<sub>6</sub><sup>3+</sup> on the CMA-functionalized Au electrode ((ii) in Fig. 3(b)). As shown in Fig. 3(b), it is also worthy to note that the observed redox currents of Ru(NH<sub>3</sub>)<sub>6</sub><sup>3+</sup> on the CMA-functionalized Au electrode are smaller than those on bare Au electrode. This suggests that the electrografted CMA layer is sufficiently covered on the Au surface enough to retard the access, and thus the electrochemical redox reactions of Ru(NH<sub>3</sub>)<sub>6</sub><sup>3+</sup> even without the electrostatic repulsion of Ru(NH<sub>3</sub>)<sub>6</sub><sup>3+</sup> from the CMA-functionalized Au surface.

### 3.3. Enhanced surface density of antibodies on G<sub>n</sub>-NH<sub>2</sub>/CMA-functionalized Au (*n* = 4 and 6)

Thus far, we have demonstrated the functionalization of Au surfaces with CMA and amine-terminated PAMAM dendrimers. As we discussed earlier, the resulting Au surfaces would be useful to immobilize sufficient amounts of antibodies, which is important to develop immunosensor Au chips with high surface density of antibodies. To confirm the usefulness of the functionalized Au to immobilize antibodies, we immobilized two different generation PAMAM

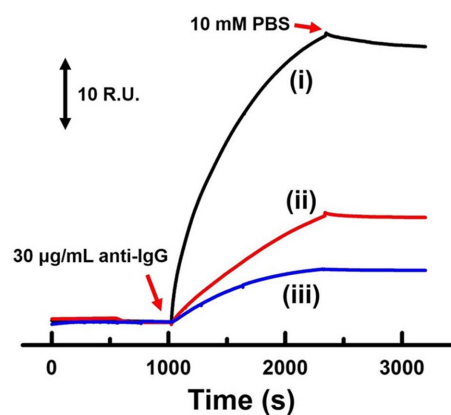


Fig. 4. SPR sensorgrams obtained on (i) a G6-NH<sub>2</sub>/CMA-functionalized, (ii) a G4-NH<sub>2</sub>/CMA-functionalized, and (iii) an ethylenediamine/CMA-functionalized Au chip when flowing 30 µg/mL anti-mouse IgG antibodies in 10 mM PBS buffer containing 1 mM NaBH<sub>3</sub>CN and subsequently washing with 10 mM PBS. Flow rate: 5 µL/min. 1 R.U. = 1 pg/mm<sup>2</sup>. M.W. of anti-IgG = 150 kDa.

dendrimers (G<sub>n</sub>-NH<sub>2</sub>, *n* = 4 and 6) onto CMA-functionalized Au chips. The resulting Au chips, i.e., G<sub>n</sub>-NH<sub>2</sub>/CMA-functionalized Au chips (*n* = 4 and 6), were then used to immobilize anti-mouse IgG antibodies via covalent cross-linkages using glutaraldehyde (see the Experimental section for experimental details, Scheme 1). We observed the amounts of anti-mouse IgG antibodies immobilized on the G<sub>n</sub>-NH<sub>2</sub>/CMA-functionalized Au chips (*n* = 4 and 6) using SPR measurements. Fig. 4 shows SPR sensorgrams obtained on the G<sub>n</sub>-NH<sub>2</sub>/CMA-functionalized Au chips (*n* = 4 and 6), indicating the immobilization of the antibodies on the functionalized Au surfaces. For comparison, a SPR sensorgram obtained on an ethylenediamine/CMA-functionalized Au chip is also presented in Fig. 4. Compared to the SPR sensorgram on the ethylenediamine/CMA-functionalized Au ((iii) in Fig. 4), the sensorgrams on the G<sub>n</sub>-NH<sub>2</sub>/CMA-functionalized Au chips (*n* = 4 and 6) indicate the immobilization of the large amounts of anti-IgG antibodies due to the high number of terminal amine groups of the dendrimers on the functionalized Au surfaces. Quantitatively, the uses of the G4-NH<sub>2</sub>/CMA-functionalized and the G6-NH<sub>2</sub>/CMA-functionalized Au chips allowed the enhanced surface density of the

immobilized anti-mouse IgG antibodies, i.e., ca.  $6 \times 10^7$  and ca.  $16 \times 10^7$  anti-IgG/mm<sup>2</sup>, respectively, compared to that (i.e., ca.  $3 \times 10^7$  anti-IgG/mm<sup>2</sup>) obtained with the ethylenediamine/CMA-functionalized Au. Based on all of the results, we concluded that the functionalization of Au surfaces with CMA and amine-terminated PAMAM dendrimers could allow high surface density of immobilized antibodies, which is an important feature for sensitive immunosensor chips.

#### 4. Conclusions

In summary, we have described a strategy for surface functionalization of Au chips with CMA and amine-terminated  $n^{\text{th}}$  generation PAMAM dendrimers ( $Gn-NH_2$ ,  $n = 4$  and  $6$ ). The surface functionalization strategy allowed high-density immobilization of antibodies on Au surfaces, which is a desirable feature for sensitive immunosensor Au chips. Especially, the functionalization of Au surfaces with CMA and  $G6-NH_2$  allowed immobilization of IgG antibodies with high surface density, which is 5 times higher than that obtained with Au surfaces with CMA and ethylenediamine. Since the high surface density of immobilized antibodies is a critical analytical feature, we believe that the suggested strategy holds great promise as a valuable way to develop sensitive immunosensor Au chips.

#### Acknowledgments

This work was supported by the National Research Foundation of Korea funded by the Ministry of Science, ICT and Future Planning (NRF-2014R1A1A2058218).

#### References

1. M. S. Wrighton, *Science*, **231**(4733), 32-37 (1986).
2. H. Randriamahazaka and J. Ghilane, *Electroanalysis*, **28**(1), 13-26 (2016).
3. B. P. Corgier, A. Laurent, P. Perriat, L. J. Blum, and C. A. Marquette, *Angew. Chem. Int. Ed.*, **46**(22), 4108-4110 (2007).
4. P. K. Ajikumar, J. K. Ng, Y. C. Tang, J. Y. Lee, G. Stephanopoulos, and H.-P. Too, *Langmuir*, **23**(10), 5670-5677 (2007).
5. K. T. Lee, J. W. Coffey, K. J. Robinson, D. A. Muller, L. Grøndahl, M. A. F. Kendall, P. R. Young, and S. R. Corrie, *Langmuir*, **33**(3), 773-782 (2017).
6. K. T. Lee, D. A. Muller, J. W. Coffey, K. J. Robinson, J. S. McCarthy, M. A. F. Kendall, and S. R. Corrie, *Anal. Chem.*, **86**(20), 10474-10483 (2014).
7. L. Sun and R. M. Crooks, *Langmuir*, **18**(21), 8231-8236 (2002).
8. S. Gan, P. Yang, and W. Yang, *Biomacromolecules*, **10**(5), 1238-1243 (2009).
9. T. H. Kim, H. S. Choi, B. R. Go, and J. Kim, *Electrochem. Commun.*, **12**(6), 788-791 (2010).
10. H. Ju, C. M. Koo, and J. Kim, *Chem. Commun.*, **47**(45), 12322-12324 (2011).
11. G. De Leener, F. Evoung-Evoung, A. Lascaux, J. Mertens, A. G. Porras-Gutierrez, N. Le Poul, C. Lagrost, D. Over, Y. R. Leroux, F. Reniers, P. Hapiot, Y. Le Mest, I. Jabin, and O. Reinaud, *J. Am. Chem. Soc.*, **138**(39), 12841-12853 (2016).
12. S. B. Lee, Y. Ju, Y. Kim, C. M. Koo, and J. Kim, *Chem. Commun.*, **49**(79), 8913-8915 (2013).
13. W. S. Yeap, M. S. Murib, W. Cuypers, X. Liu, B. van Grinsven, M. Ameloot, M. Fahlman, P. Wagner, W. Maes, and K. Haenen, *Chem. Electro. Chem.*, **1**(7), 1145-1154 (2014).
14. M. Delamar, R. Hitmi, J. Pinson, and J. M. Saveant, *J. Am. Chem. Soc.*, **114**(14), 5883-5884 (1992).
15. B. P. Corgier, C. A. Marquette, and L. J. Blum, *J. Am. Chem. Soc.*, **127**(51), 18328-18332 (2005).
16. Y. Kim and J. Kim, *Anal. Chem.*, **86**(3), 1654-1660 (2014).
17. S. B. Lee, J. Kwon, and J. Kim, *Electroanalysis*, **27**(9), 2180-2186 (2015).
18. J. Yoon, T. Cho, H. Lim, and J. Kim, *Anal. Bioanal. Chem.*, **408**(25), 7165-7172 (2016).
19. J. M. Kim, H. Ju, H. S. Choi, J. Lee, J. Kim, J. Kim, H. D. Kim, and J. Kim, *Bull. Korean Chem. Soc.*, **31**(2), 491-494 (2010).
20. M. Tencer, O. Krupin, B. Tezel, and P. Berini, *J. Electrochem. Soc.*, **160**(1), H22-H27 (2013).
21. B. P. Corgier, S. Bellon, M. Anger-Leroy, L. J. Blum, and C. A. Marquette, *Langmuir*, **25**(16), 9619-9623

- (2009).
22. C. A. Mandon, L. J. Blum, and C. A. Marquette, *Chem. Phys. Chem.*, **10**(18), 3273-3277 (2009).
23. N. B. Li and J. Kwak, *Electroanalysis*, **19**(23), 2428-2436 (2007).
24. S. Watanabe and S. L. Regen, *J. Am. Chem. Soc.*, **116**(19), 8855-8856 (1994).
25. M. Nemanashi and R. Meijboom, *Langmuir*, **31**(33), 9041-9053 (2015).
26. S. W. Svenningsen, A. Janaszewska, M. Ficker, J. F. Petersen, B. Klajnert-Maculewicz, and J. B. Christensen, *Bioconjugate Chem.*, **27**(6), 1547-1557 (2016).